Preparation and analysis of superconducting Nb-Ge films

L. R. Testardi, R. L. Meek, J. M. Poate, W. A. Royer, A. R. Storm, and J. H. Wernick
Bell Laboratories, Murray Hill, New Jersey 07974
(Received 26 December 1974)

The dependences of T_c, resistivity, resistance ratio, and structure on chemical composition and sputtering conditions for Nb-Ge films have been studied. The chemical composition, impurity content, and x-ray structure were obtained using Rutherford backscattering, nuclear techniques, and x-ray diffraction. Although T_c varies with composition, it is not found to be critically dependent upon exact stoichiometry; the Nb/Ge ratios vary by $\sim 13\%$ (2.6 to 3) for films with ~ 23-K onsets and by $\sim 40\%$ (2.2 to 3.3) for films with ~ 20-K onsets. For compositions similar to the bulk, the films have comparitively much higher T_c's and smaller lattice parameters. X-ray results show the films to contain predominately A-15 phase (except for Nb/Ge $\lesssim 2.5$) with lattice parameters varying from 5.15 Å for Nb-rich low-T_c films to 5.12 Å for Ge-rich films. Several percent of oxygen and carbon occur in low-T_c amorphous films deposited at 650 °C but this is considerably reduced in high-T_c films made simultaneously at ~ 750 °C. No argon was found and the nitrogen content was generally less than 1%. No correlation of high T_c's and impurities was found. The optimum deposition temperature and resistivity are lowest, and the resistance ratio highest for Nb/Ge ratios somewhat below 3/1. A simple correlation of T_c and resistance ratio is reported which is largely independent of all sputtering conditions and composition and which suggests that slightly higher T_c's may be possible. Negative bias was found to be detrimental to T_c while positive bias had relatively little effect. Magnetic-field-assisted sputtering led to significant increases in the sputtering rate and the optimum deposition temperature.

I. INTRODUCTION

A. Background

Most high-temperature superconductors exhibit some form of structural instability.[1] These instabilities, evidence now warrants, are indeed probably the cause of the high T_c's—a conjecture which has lead to new efforts to obtain unstable or metastable phases in a search for better superconductors. Mo-Re alloys sputtered at the eutectoidal decomposition temperature have yielded a new superconducting phase with significantly enhanced T_c relative to the bulk phase.[2] A search for metastable phases in about 40 other alloys prepared by sputtering onto hot substrates has shown that such phases can be readily obtained by this method and that these often show an enhanced T_c.[3] Recently, Gavaler[4] obtained T_c onsets of 22.3 K in films of Nb-Ge (bulk $T_c \sim 6$ K) sputtered onto hot substrates in a high argon pressure. This important result marked the first increase in the maximum known T_c in about four years. Subsequently, Testardi *et al.*[5] reproduced these results and obtained films with T_c onsets of ~ 23 K (and now also reported by Gavaler *et al.*[6]). In this work it was conjectured that (i) the high-T_c phase was detrimentally affected by the presence of high-energy particles present under normal sputtering conditions (and which are reduced in high argon pressure) and (ii) the growth of high-T_c films is relatively insensitive to large ($\sim 25\%$) variations in the overall Nb/Ge ratio of the target.

The importance of high-energy particle damage to the high-T_c phase was concluded from studies of the dependence of T_c on argon pressure and sputtering voltage. Chencinski and Cadieu[7] and Ghosh *et al.*[8] have now also sputtered high-T_c Nb-Ge films and reached similar conclusions on the detrimental effects of these high-energy particles.

The question of how sensitive the T_c of Nb-Ge is to composition near the exact stoichiometric ratio 3/1 has attracted considerable comment but, as yet, no quantitative answers. Carpenter and Searcy[9] were the first to synthesize and identify A-15–structure Nb-Ge, and Geller[10] was the first to recognize that the compound normally grown to be Nb_3Ge was, in fact, nonstoichiometric. Later, Matthias *et al.*[11] splat-cooled the approximate Nb_3Ge and obtained a very broad superconducting transition beginning at ~ 17 K. The high T_c was assumed to result from the nearly exact stoichiometric Nb_3Ge obtained by the rapid-quench preparation compared to the bulk compound, where the Nb/Ge ratio is ~ 3.3[12] to 4.[13]

The major content of this paper is devoted to the identification of the chemical composition, crystal structure, and impurity content of high-T_c Nb-Ge sputtered films. The method for determining the absolute chemical composition is the Rutherford backscattering technique—an analytical tool ideally suited to perform this unambiguously and without the need or uncertainties of secondary standards. The studies of T_c, composition, and crystal struc-

ture have been performed over a wide range in composition (Nb/Ge ratio from ~2 to 5.5) and also as a function of some of the variables available to the sputtering deposition process. The results provide an informative, and sometimes surprising, picture of what makes high-T_c Nb-Ge. On the first premise—that high-energy sputtering particles can be bad for T_c—we also give the results of some abbreviated but relevant studies of films sputtered with substrate bias and with magnetic fields. The studies of chemical composition show that T_c does depend on the Nb/Ge ratio, but not in the crucial manner expected for exact stoichiometry. The occurrence of impurities varies in an unexpected way with sputtering conditions but does not correlate with the occurrence of high T_c's. Finally, a simple correlation between resistance ratio and T_c is pointed out. This relation is remarkably insensitive to sputtering conditions and to composition. It may be partially rooted in structural order or defects—a significant part of the puzzle at hand for which quantitative results are not yet available. From this correlation there seems to be an indication that slightly higher T_c's may yet be possible.

B. Analytic techniques for thin film

The Nb-Ge films of interest here present a clear demonstration of the need for quantitative information on their composition. There are generally[14] two types of experimental approaches to the problem of thin-film-composition determination: first, surface sensitive techniques where depth information or profiling is accomplished by sputter sectioning, and, second, the nuclear techniques employed here.

The surface techniques such as Auger spectroscopy are sensitive probes of the outermost surface layers. Sectioning or profiling is usually accomplished by means of sputtering material away. As the sputtering process in the case of a polycrystalline alloy is not yet fully understood, surface techniques used in combination with sputtering may measure surface compositions that are not representative of the bulk material. Nuclear techniques, in particular Rutherford scattering, that use energetic ion beams can provide quantitative information on film composition in a nondestructive fashion. As usually performed, however, their depth resolution is ~100 Å. It is evident that no single technique provides complete information, and here we employ Rutherford scattering for compositional analysis and x-ray diffraction for structural analysis. A nuclear microanalysis method is employed to obtain a quantitative estimation of N in the films.

II. EXPERIMENTAL

A. Film deposition

Films were deposited by dc getter sputtering in a system described by Theurer and Hauser[15] and shown in Fig. 1. Getter sputtering is performed in a closed liquid-nitrogen-cooled can whose inside surface is continually being sputter coated with the material being deposited. The gettering action of the cold fresh-sputtered surfaces leads to a considerable improvement in the purity of the environment and the films. The sputtering was carried out in either of two vacuum systems where the initial pumpdown pressures varied from 5×10^{-5} to 5×10^{-9} Torr, and with leak and outgassing rates differing by factors of typically 30 and sometimes exceeding 200. In one of the vacuum systems (with Vac-sorb roughing and Vac ion pumping) equipped with a mass-spectrometer the major outgas and leak constituents (with heated substrates) were found to be hydrocarbons, H, He, and a constituent with mass 28 (probably CO but possibly N_2).

All sputtering has been done with 99.9999% pure argon in a dynamically pumped system. Substrates were generally sapphire (Al_2O_3), but occasionally MgO, spinel, and graphite were used. Substrate heating was obtained by passing up to 150 A (60 Hz)

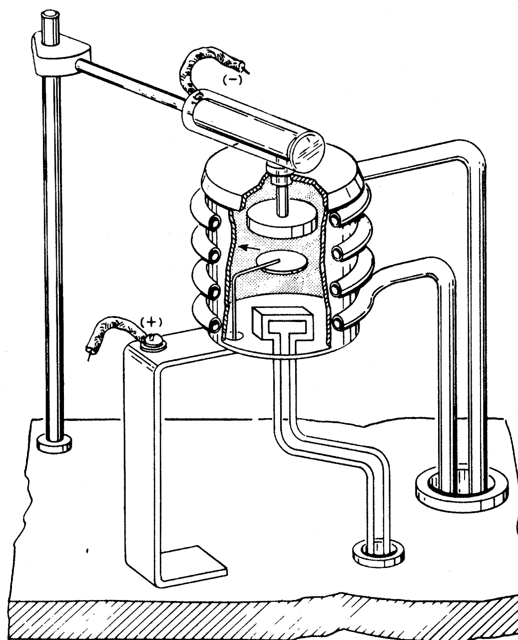

FIG. 1. Getter-sputtering apparatus of Theurer and Hauser (Ref. 15). Liquid nitrogen is passed through the cooling coils surrounding the can. The substrates sit on a tantalum sheet table. The table is constructed to allow resistive heating with a temperature differential of ~100 °C across five substrates.

through a tantalum sheet table on which the substrates were resting. An additional shunting strap of tantalum, welded to the bottom of the table, was added to establish a temperature differential of ~100°C across the table. The table held approximately five or six substrates; so each film differed in deposition temperature by ~20°C. The table temperature was measured from below (target above) using a Pt–vs–Pt-Rh thermocouple. From independent pyrometer and surface-thermocouple measurements it was determined that the film surface temperature during deposition was ~150± 50°C below that given by the underside thermocouple. It is the estimated film surface temperature (called T_D) which is used for all discussion below.

B. Thickness and resistance measurements

Film thicknesses (± 15%) were determined from weight-gain measurements of the substrates by using the approximate density 8.7 g/cm^3. Rutherford scattering permits an accurate determination of the surface density (i.e., number of atoms per cm^2), and, assuming a bulk density, the linear thickness can also be calculated. Standard four-probe ac resistance measurements were made using pressure contacts. Temperatures were measured to an accuracy of ~± 0.2°K with calibrated carbon and germanium resistors and/or a silicon diode.

C. Target preparation

Sputtering targets were made by arc casting the elements in the desired ratio. The Ge was semiconductor grade while the Nb, as purchased, was specified at > 99.9% purity. When later analysis revealed large quantities of carbon and oxygen in some of this material an ingot was zone refined by K. Bachman and J. Rubin at Bell Labs to yield (99.99–99.999)% purity. (No large changes in properties resulted.) Most of the studies of compositional variation were performed starting with a target of Nb_5Ge_3 around which were added turns of Nb wire to increase the Nb/Ge ratio. (The purity of this Nb wire was not known.) The diameter of the targets ranged from 2 to 4 cm.

D. X-ray measurements

X-ray diffraction data for the superconducting films were generally obtained by use of a wide-film Debye camera and Cu$K\alpha$ radiation. This camera uses 5×7-in. film which allows the detection of diffracting planes having preferred orientation at a considerable angle to the plane of the sample substrate. Our samples were held inclined to the x-ray beam at an angle of 18°. This angle allows a fairly large section of the sample to be covered by the beam, while not cutting off too much of the forward reflection region. Some diffractometer traces of the films were also taken using a GE SPG-1 apparatus.

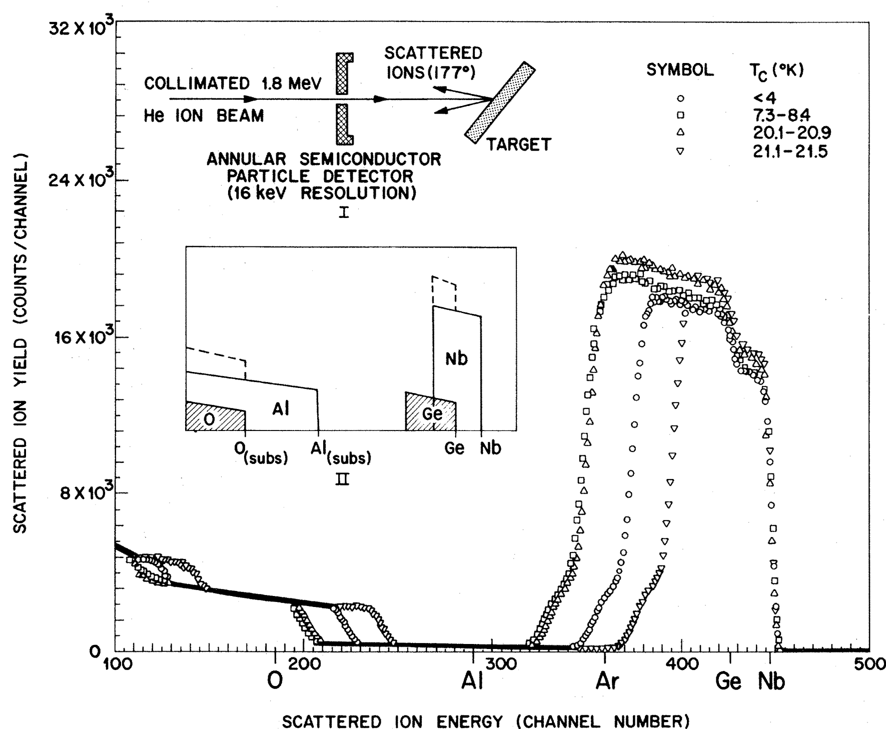

FIG. 2. (I) Schematic representation of Rutherford backscattering experiment, (II) idealized backscattering spectrum. Also shown are data for four films made simultaneously with T_D between 640 °C and 740 °C and having T_c's between <4.2 and ~21.5 K.

One of the arc-melted Nb_5Ge_3 targets was also examined along a transverse section of the button by means of powder x-ray techniques (Straumanis camera-114.6 mm diameter-Cu radiation). This was shown to be uniform consistent with the congruent nature of this phase, and to exhibit the tetragonal $D8m$ structure.[16] The observed and calculated d spacings and intensities were in reasonable agreement with published values[13] and yielded $a_0 = 10.163$ Å, $c_0 = 5.130$ Å, with position parameters $x = 0.074$, 0.17 and $y = 0.223$.

E. Rutherford scattering

Backscattering of high-energy (MeV) He^+ ions has proven to be a very valuable technique for elucidation of surface, interface, and thin-film phenomena.[17,18] A typical experimental arrangement is shown schematically as insert I to Fig. 2. A beam of 1.8-MeV He^+ ions is passed through two Ta collimators 1 mm in diameter about 2 m apart. The backscattered He ions (at ~177°) are detected by an annular 50-mm^2 silicon-surface barrier detector having an energy resolution of ~15 keV. Secondary-electron suppression, dead-time correction, and pileup rejection electronics are used. The typical chamber vacuum, beam current, and He ion fluence are 10^{-6} Torr, 5 nA, and 10^{16} cm^{-2}, respectively.

The interaction between He ions, in this energy regime, and the solid can be separated into the ion-nucleus interaction (scattering) and the ion-electron interaction (energy loss).

Scattering obeys the classical Rutherford law; so the laboratory differential scattering cross section is given by

$$\sigma(\theta_L) = 1.296\times 10^{-27}(Z_1 Z_2/E_0)^2 \times [\csc^4(\tfrac{1}{2}\theta_L) - 2(M_1/M_2)^2 + \cdots] \text{ cm}^2/\text{srad}, \quad (1)$$

where $Z_1(M_1)$ is the atomic number (mass) of the incident particle, $Z_2(M_2)$ is the atomic number (mass) of the scattering nucleus, E_0 is the incident particle energy in MeV, and θ_L is the laboratory scattering angle. The next term in the expansion is of order $(M_1/M_2)^4$ and may usually be neglected.

Since the scattering is elastic, conservation of energy and momentum yield

$$\frac{E}{E_0} = \left(\frac{M_1}{M_1+M_2}\right)^2 \left[\cos\theta_L + \left(\frac{M_2^2}{M_1^2} - \sin^2\theta_L\right)^{1/2}\right]^2 \equiv K(M_2), \quad (2)$$

where E_0 and E are the incident and emergent laboratory energies of the scattered particle. Since M_1 and θ_L are fixed, the energy of the backscattered ion depends on the mass M_2 of the scattering atom; that is, the energy of the backscattered ion identifies the mass of the atom from which it scattered.

Thus far, energy loss as the incident particle penetrates the solid has been neglected. At these energies, an ion traversing a solid will only lose energy to the electrons of the solid. For scattering from atoms of a given mass, the scattered-ion energy scale may be converted to a depth scale through

$$\Delta t = \Delta E\left(K(M)\left.\frac{dE}{dx}\right|_{\text{in}} + \frac{1}{|\cos\theta_L|}\left.\frac{dE}{dx}\right|_{\text{out}}\right)^{-1}, \quad (3)$$

where Δt is the depth increment, ΔE is the energy shift, and dE/dx is the average (electronic or inelastic) energy loss per unit path length.

For definiteness, consider scattering of 1.8-MeV incident He^+ ions from an ~1000-Å-thick film of uniform Nb_3Ge on an Al_2O_3 substrate. An idealized spectrum is shown as insert II to Fig. 2. The energies for ions scattered from Ge and Nb at the surface are noted on the energy axis, 1.44 and 1.52 MeV, respectively. The scattered ions with the highest energy are those from Nb at the surface. A continuous spectrum of scattered ions at lower energies is observed because of scattering from Nb atoms deeper in the film [Eq. (3)] which terminates at a lower energy corresponding to scattering from Nb atoms at the substrate-film interface. Note that the number of ions scattered from Nb atoms increases with depth owing to the lower energy and consequently greater cross section [Eq. (1)] for the scattering event.

Scattering from Ge atoms at the surface corresponds to a lower energy than for surface Nb atoms [Eq. (2)], but to a higher energy than for scattering from Nb atoms at the substrate interface. Thus there is an energy overlap for ions scattered from Nb and Ge. The resulting composite spectrum appears as shown by the dotted line in insert II to Fig. 2.

Finally, the spectrum edges corresponding to Al and O for the sapphire substrate are shifted down in energy with respect to the energy positions corresponding to Al and O at the surface because of energy loss as the incident ions penetrate through and exit from the overlying Nb_3Ge film. From this shift it can be (and has been) determined that little or no diffusion of Al or O from the substrate into the film has occurred.

III. RESULTS

A. Ion-scattering results

Scattered-ion spectra, for the same (dead-time corrected) integrated number of incident ions, from four of six samples deposited in the same

run (as described in Sec. II A), are shown in Fig. 2. The Nb/Ge ratio is obtained from the scattered-ion yields, Y(counts/channel), by use of

$$\frac{N_{\mathrm{Nb}}}{N_{\mathrm{Ge}}}=\frac{\sigma_{\mathrm{Ge}}}{\sigma_{\mathrm{Nb}}}\frac{Y_{\mathrm{Nb}}(K_{\mathrm{Nb}}+|\sec(\theta_L)|C_{\mathrm{Nb}})}{Y_{\mathrm{Ge}}(K_{\mathrm{Ge}}+|\sec(\theta_L)|C_{\mathrm{Ge}})}, \quad (4)$$

obtained by combining Eqs. (1) and (3), where

$$C=\left.\frac{dE}{dx}\right|_{\mathrm{out}}\Big/\left.\frac{dE}{dx}\right|_{\mathrm{in}} . \quad (5)$$

Equation (4) is independent of the need for accurate knowledge of dE/dx as a function of energy, which is generally only known to $\pm 10\%$, but depends only on knowledge of the shape of the stopping-power curve, which is quite well known. Furthermore, dE/dx varies only slowly with energy for the present case, so the C's are ~ 1. The relative Nb/Ge compositions of the samples shown in Fig. 2 are listed in Table I along with the estimated uncertainty, which comes largely from deconvolution of the Nb and Ge spectra.

Figure 2 also shows a significant variation in sample thickness (a factor of 2), with the two end samples being thinner than those in the middle of the substrate table. The thinnest sample shows no evidence of Ar incorporation, and Ar has never been detected. (The estimated sensitivity for argon detection in these films is 10^{16} cm^{-2}.) Point-to-point scans showed no stoichiometry differences on a sample, and there is no evidence for change in Nb/Ge ratio with depth into the films.

B. X-ray results

Table II contains a listing of the critical temperatures, sputtering conditions, and lattice parameters of the A-15 phase obtained by sputtering from targets of differing average compositions. The average lattice constants were computed from the diffraction lines for 2θ greater than 107°, i.e., beginning with the 520/432 reflections. Reflections were observed through $2\theta \cong 135°$ (611/532), the second most intense line. For the highest T_c films it was sometimes possible to detect the α_1-α_2 doublet (Cu$K\alpha$ radiation) at $2\theta \approx 135°$.

The lattice parameters were found to decrease with decreasing Nb/Ge ratio. For an Nb/Ge ratio of ~ 3, where T_c's are highest, $a_0 \sim 5.13 \pm 0.01$ Å, which is considerably less than the value ~ 5.17 Å obtained for bulk A-15 Nb-Ge. This result is in general agreement with the previous findings of Gavaler,[4] Chencinski and Cadieu,[7] and Pendrys et al.[8] The large lattice parameter of the bulk material was the prime indicator that its composition was nonstoichiometric.[10] Note, however, that films prepared with the bulk composition Nb/Ge ~ 4 have, in fact, considerably smaller lattice parameters than that of the bulk. The pronounced difference between bulk and film Nb-Ge at the same composition is more clearly demonstrated in the superconducting T_c's (see below). All lattice-parameter measurements have been made for films on the substrate. The effect of substrate strains, discussed below, is not known.

X-ray studies show that in the approximate compositional range Nb/Ge ~ 2.6 to 5.5 the films yield predominantly single-phase A-15 material. The very weak second-phase lines observed in these films have been estimated (from line-intensity–exposure-time relations and from independent measurements of small amounts of Nb in bulk Nb_5-Ge_3) to correspond to less than 5% second phase. Thus the Rutherford determination of average Nb/Ge composition is essentially correct in describing the A-15 phase composition.

As expected, the width of the single-phase A-15 region in Nb-Ge is considerably enhanced in the films which are deposited below 1000°C, relative to bulk samples formed at high temperatures. (Similar conclusions appear also true for the $D8m$ phase where the Nb-rich phase boundary for the films is found at Nb/Ge ~ 2 while occurring at smaller values in the bulk compound.) This is no doubt an important[19] but, as shown below, not the controlling factor in obtaining high T_c's.

C. Impurity content

There are a variety of ways of determining impurity content in these films. An overall estimate of gross impurity content can be made by compar-

TABLE I. Nb/Ge ratio and impurity content factor for typical films. The estimated upper limit of total impurity concentration, relative to Nb, is given in column 6.

Sample No.	T_D (°C)	T_c (K)	$N_{\mathrm{Nb}}/N_{\mathrm{Ge}}$	N_{Nb} (atoms/cm^2)	$\sum_i \frac{N_i[\epsilon_i]}{N_{\mathrm{Nb}}[\epsilon_{\mathrm{Nb}}]}$
750/1	640	<4.2	3.21 ± 0.1	1.0×10^{18}	0.11
750/2	660	8.4–7.3	2.97 ± 0.1	1.4×10^{18}	0.08
750/4	700	20.9–20.1	2.99 ± 0.1	1.5×10^{18}	0.02
750/6	740	21.5–21.1	3.10 ± 0.1	0.8×10^{18}	0.01

TABLE II. Summary of critical temperature and x-ray data for sputtered Nb-Ge films. V: Very; W: Weak. T_D is deposition temperature (±50 °C uncertainty); V is the sputtering voltage, P is the argon pressure (uncorrected thermocouple gauge reading); and t is the approximate film thickness.

Sputtering conditions	Nb/Ge ratio	T_c (°K) start	T_c (°K) end	a_0 (Å) for the A-15 phase	Remarks
$T_D \sim 800$ °C $V = 600$ $P = 200$ mTorr $t \sim 2000$ Å	5.52	9.6	7.3	$5.151\left\{\begin{matrix}+0.009\\-0.013\end{matrix}\right.$	A-15 Two VVW extra lines; one attributed to Nb_5Ge_3 and the other to Nb.
$T_D \sim 760$ °C $V = 600$ $P = 200$ mTorr $t \sim 2900$ Å	4.1	13.4	11.8	$5.141\left\{\begin{matrix}+0.019\\-0.020\end{matrix}\right.$	A-15 One VVW extra line attributed to Nb.
$T_D \sim 740$ °C $V = 600$ $P = 200$ mTorr $t \sim 2900$ Å	3.3	20.5	19.6	$5.128\left\{\begin{matrix}+0.013\\-0.009\end{matrix}\right.$	A-15 No extra lines observed.
$T_D \sim 740$ °C $V = 600$ $P = 300$ mTorr $t \sim 2000$ Å	3.11	21.5	21.1	5.138 ± 0.001	A-15 Diffractometer trace (started at $hkl = 210$). No extra lines observed.
$T_D \sim 740$ °C $V = 600$ $P = 200$ mTorr $t \sim 3000$ Å	3.05	23.0	22.0	5.128 ± 0.007	A-15 Several VVW extra lines.
$T_D \sim 740$ °C $V = 600$ $P = 200$ mTorr $t \sim 2400$ Å	2.74	22.0	20.3	$5.123\left\{\begin{matrix}+0.007\\-0.013\end{matrix}\right.$	A-15 Three VVW extra lines attributed to Nb_5Ge_3 and one VVW line attributed to Nb.
$T_D \sim 720$ °C $V = 600$ $P = 200$ mTorr $t \sim 2000$ Å	2.6	23.2	21.9	$5.133\left\{\begin{matrix}+0.005\\-0.006\end{matrix}\right.$	A-15 Three VW-VVW extra lines attributed to Nb_5Ge_3. the order of intensities as expected.
$T_L \sim 780$ °C $V = 800$ $P = 200$ mTorr $t \sim 3000$ Å	2.16	19.7	15.0	$5.12\left\{\begin{matrix}+0.02\\-0.04\end{matrix}\right.$	Two phases: A-15 + Nb_5Ge_3.
$T_D = 760$ °C $V = 800$ $P = 200$ mTorr $t \sim 1500$ Å	1.98	12.8	4.4	$5.16\left\{\begin{matrix}+0.02\\-0.01\end{matrix}\right.$	$D8m$ structure. VW extra diffraction lines attributed to presence of A-15
$T_D = 740$ °C $V = 800$ $P = 200$ mTorr $t \sim 3500$ Å	1.96	19.6	13.5	5.13 (based only on the A-15 321 reflection. Higher angle A-15 lines absent on this pattern).	$D8m$ structure. W extra lines attributed to A-15 and Nb.

ing the scattered-ion yield from Nb and Ge in the film to the yield obtained from pure (i.e., elemental) Nb and Ge. It can be shown (assuming Bragg's Law[20]) that

$$\frac{Y^0_{Nb}}{Y_{Nb}} = 1 + \frac{N_{Ge}[\epsilon^{Nb}_{Ge}]}{N_{Nb}[\epsilon^{Nb}_{Nb}]} + \frac{\sum_i N_i[\epsilon^{Nb}_i]}{N_{Nb}[\epsilon^{Nb}_{Nb}]} , \qquad (6)$$

where Y^0_{Nb} is the yield from pure Nb and $[\epsilon]$ is the atomic stopping cross-section factor[20] defined by

$$[\epsilon] = (K\epsilon_{in} + |\sec\theta_L|\epsilon_{out}), \qquad (7)$$

where the unbracketed ϵ's are the atomic stopping cross section for the species in question. The superscripts in the atomic stopping cross-section factors refer to the scattering nucleus and the subscripts to the stopping material. N_i in Eq. (6) is the number of impurity atoms i per unit volume. In fact one can estimate the Nb/Ge ratio from Eq. (6), but this is inaccurate because of uncertainty in the appropriate ϵ's and impurity content N_i. The Nb-Ge ratio is determined most accurately from Eq. (4).

An estimate of the upper limit to the impurity term $(\sum_i N_i[\epsilon_i])/N_{Nb}[\epsilon^{Nb}_{Nb}]$ for the four films from Fig. 2 is given in Table I. N_{Ge}/N_{Nb} was determined from Eq. (4), and Y^0_{Nb}/Y_{Nb} was determined experimentally from measurements of the films and a cold-worked sample of pure Nb. The stopping cross-section factors were derived from the compilation of Northcliffe and Schilling.[21] To first approximation it may be assumed that

$$\Big(\sum_i N_i[\epsilon_i]\Big)\Big/N_{Nb}[\epsilon_{Nb}] \approx \Big(\sum_i N_i\Big)\Big/N_{Nb} . \qquad (8)$$

These upper limits were calculated by assuming uncertainties in the stopping cross-section factors of ~10%. The variations of the Nb and Ge scattered-ion yields (Y_{Nb} and Y_{Ge}) for the four films of Fig. 4 are therefore due to the presence of impurities in the films and variations in composition.

It is clear from Fig. 2 that such small amounts of light impurities (C, O, or N, say) would not be detectable for films on sapphire substrates because the scattered-ion yield from any such light impurity would be obscured by the large scattered-ion background from the substrate. Films were therefore grown on graphite substrates to examine this question.

Films deposited on graphite had T_c's considerably degraded (19 K was highest) and with very broad superconducting transitions compared to those deposited on sapphire. The difference may result from large thermal-expansion differences or from the small surface flaking which occurs with the graphite substrates.

For films deposited on graphite (basal) plane substrates an unusual behavior was also found. Although the graphite and normal-state film conductances were not grossly different, superconductivity could only be observed when the measuring probes were on the film side of the substrate. When the substrate, which was ~0.5 mm thick, was turned over no evidence of superconductivity (to within ~1% in measured resistance) was observed. This result no doubt reflects the extreme tendency for two-dimensional current flow in graphite.

Figure 3 is a typical spectrum obtained from a film on a graphite substrate. O and C at the film surface are readily apparent (~10^{16} cm^{-2} or several monolayers), and the bulk O and C content can be estimated as indicated in the figure. These estimates must be regarded as upper limits because of uncertainty in the extrapolations of the low-energy scattered-ion "tail" from the film, which is probably due to slit-scattering or similar effects. Results are given in Table III. It appears that the O and C contents are of the order of a few atomic percent at most and that the impurity content decreases with increasing T_c. Note that there is no evidence for N (N/Nb< 0.01) in the films on graphite substrates. Finally, the high T_c's do not correlate (to within several K) with the occurrence of any impurity detected.

D. Determination of nitrogen content

The backscattering data for films deposited on carbon substrates show that while C and O can be incorporated in the films at the percent atomic level there is no evidence of nitrogen. The fact that NbN is a superconductor with a high T_c stimulated us to examine the films deposited on sapphire for N content. As backscattering is not suitable for the direct observation of light impurities in the Nb-Ge films on sapphire we employed the $^{14}N(d,\alpha)^{12}C$ nuclear reaction which is highly exoergic, with a Q value of +13.6 MeV.

Incident deuteron energies of 1 MeV were used, and the α particles from the reactions were detected in an annular solid-state detector. Figure 4 shows spectra from a calibration Si_3N_4 sample (500 Å thick) and a Nb-Ge film. The energy of the α_0 group is 9.7 MeV. However, the face of the detector was covered with a 19-μm Mylar foil to stop the backscattered deuterons from entering the detector. The α_0 particles lose approximately 1.35 MeV penetrating the foil.

The nitrogen content of the film was estimated directly by comparison with the calibration Si_3N_4 sample. Runs were taken for the same number of incident deuterons. The integrated counts in the α_1 and α_0 peaks (Fig. 4) for the Si_3N_4 calibration sample are 1010 and 63, respectively, where the

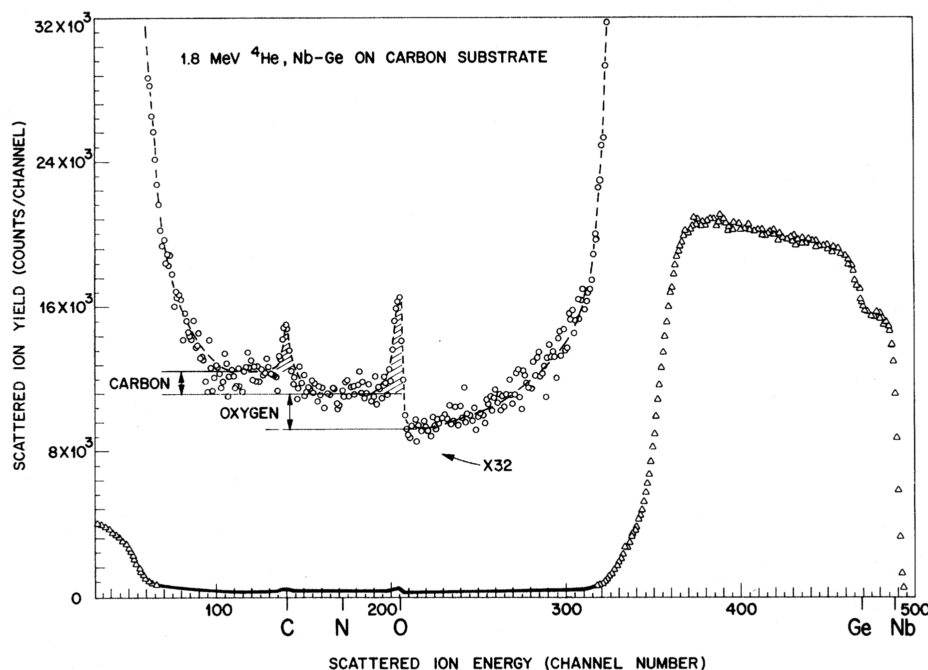

FIG. 3. Rutherford backscattering spectrum for Nb-Ge film deposited on graphite substrate.

corresponding counts to the Nb-Ge films are 48 and 3, respectively. This film gave the highest level of N impurity. Table IV shows the N impurity content of a series of film on sapphire calculated assuming the density of the 500-Å Si_3N_4 film to be 3.2 g/cc. The values of the impurity content in Table IV represent the total number of N atoms in or on the films.

E. Compositional dependence of T_c

An important question concerning the superconductivity of sputtered Nb-Ge films is how critically do the high T_c's depend upon achieving exact stoichiometry. Figure 5 shows the variation of T_c with Nb/Ge ratio as determined from Rutherford backscattering analysis. For Nb/Ge ratios between ~2.4 and 3.2 there was considerable effort in achieving the optimum deposition conditions. Also, within this range, we give the results for some films made under nonoptimum conditions—usually those obtained with T_D's about 50–100°C too low—which produced the low T_c data points. Outside of this compositional range the sputtering conditions were nearly optimum except for the sputtering voltage, which, on some occasions, may have been somewhat too high. Thus T_c's on the sides of the maximum shown might still be increased somewhat but probably by an insignificant amount. This would, in no way, alter the conclusions to follow.

The data show that, although the highest T_c's do fall in the compositional range Nb/Ge ~ 2.6–3.3, they do not show the critical dependence on composition (say, roughly several percent) which one might expect to attribute to perfect stoichiometry. Indeed, films with T_c onsets of ~ 23 K occur over a ~ 13% range in composition (Nb/Ge ~ 2.6–3), and films with T_c onsets above 20 K can be found over an ~ 40% variation (Nb/Ge ~ 2.2–3.3).

It is important to note that over most of this range (Nb/Ge ~ 2.6–5.5) x-ray diffraction showed only very weak second phases, which have been

TABLE III. Probable upper limits of C and O content in films grown on graphite substrates.

Sample No.	T_c (K)	Nb/Ge	N_{Nb} (atoms/cm^2)	C/Nb	O/Nb
700/1	<4.2	3.24	2.2×10^{18}	0.12	0.11
700/2	10.5	3.05	2.4×10^{18}	0.06	0.03
700/3	17.5	2.71	2.5×10^{18}	0.12	0.01
700/4	18.6	3.12	2.2×10^{18}	0.07	0.02
700/5	12.9	2.94	1.5×10^{18}	···	0.06

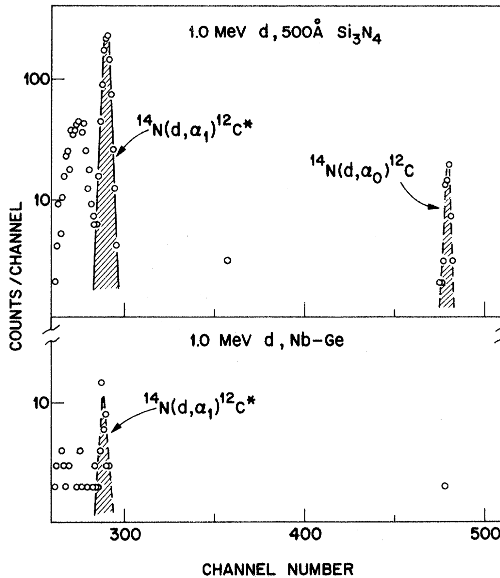

FIG. 4. (d, α) nuclear reaction spectrum for a Si_3N_4 standard and a Nb/Ge film. The reaction is used to determine the N content of the films.

estimated by separate calibration (see Sec. III H) to be less than 5%. Thus the T_c dependence on composition represents predominantly the single A-15 phase behavior.

Further insight into compositional effects and film behavior comes from comparing the data of Fig. 5 with those obtained in the bulk. According to several authors[12,13] the A-15 phase in bulk material forms at Nb/Ge ~ 3.3 or 4. Figure 1 shows that sputtered films at Nb/Ge ~ 4 would yield T_c's of approximately 14 K, which is considerably in excess of ~ 6 K obtained in the bulk. Thus the significantly higher T_c's obtained in the films cannot be due to stoichiometry alone. Furthermore, since the bulk composition is nonstoichiometric, one cannot naively argue the presence of good ordering in the films without further identifying how such order occurs at this composition. Indeed, nowhere in our compositional range are T_c's found to be as low as that of the bulk.

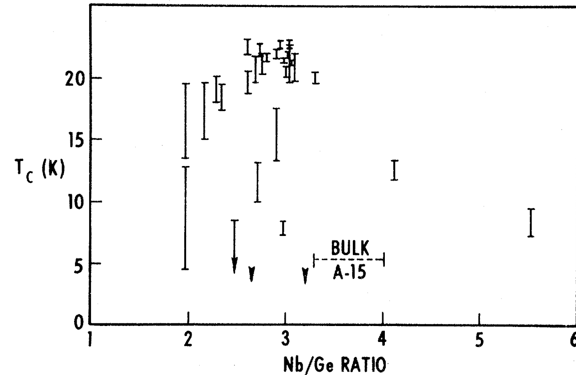

FIG. 5. Variation of T_c with Nb/Ge ratio.

Critical current measurements (to be published) also show that for films of all compositions having the A-15 structure the superconductivity is bulklike rather than filamentary for all T up to the reported T_c.

A further point which deserves note concerns the shape of the trend shown in Fig. 5. Since the films have mainly the A-15 phase we might assume that for Nb/Ge > 3 the excess Nb atoms are on the Ge sublattice, with the converse for Nb/Ge < 3. Since the integrity of the A(Nb) chains is generally felt to be most important for T_c in this A_3B structure, one expects, and often finds, that with compositional variation T_c is reduced more drastically with disorder on A chains (e.g., with Nb/Ge < 3) than on B sites. Figure 5 shows that this simple concept fails in the sputtered films. The failure may lie in the assumption that the only microscopic change occurring with compositional variation is to progress from excess A atoms randomly occurring on B sites to the inverse situation.

F. Compositional dependence of optimum T_D and electrical resistivity

Figure 6 shows how the optimum value of T_D varied with chemical composition over the range Nb/Ge ~ 2–5.5. The error in determining T_D is ~± 50°C, and the optimum value, which may de-

TABLE IV. Results of nitrogen determination in Nb-Ge films.

Sample No.	T_c (K)	Nb/Ge	No. of N atoms/cm	No. of Nb atoms/cm^2	N/Nb ratio
800/5	21	2.71	$(12\pm2)\times10^{15}$	2.9×10^{18}	4.10×10^{-3}
750/1	<4.2	3.21	$(5\pm1)\times10^{15}$	1.0×10^{18}	5.10×10^{-3}
750/2	8.4	2.97	$(4\pm1)\times10^{15}$	1.4×10^{18}	2.8×10^{-3}
750/3	19.4	2.93	$(4\pm1)\times10^{15}$	1.4×10^{18}	2.8×10^{-3}
750/4	20.9	2.99	$(7\pm1)\times10^{15}$	1.5×10^{18}	4.7×10^{-3}
750/5	21	2.67	$(3\pm1)\times10^{15}$	1.3×10^{18}	2.3×10^{-3}
750/6	21.5	3.10	$(2\pm1)\times10^{15}$	0.8×10^{18}	2.5×10^{-3}

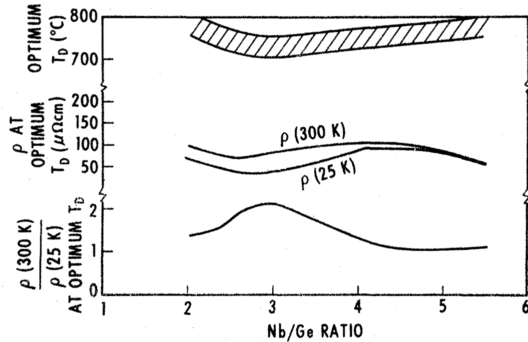

FIG. 6. Variation of optimum T_D, electrical resistivity and resistance ratio with Nb/Ge content.

pend somewhat on sputtering conditions and geometry, cannot be defined to much better than 50°C. The relative measurements given in Fig. 6, however, are sufficiently reliable to establish the trend shown. A minimum in the optimum T_D occurs for Nb/Ge in the interval ~2.7–3, with T_D rising only slowly on either side of this range. The lowest optimum T_D's occur in the same compositional range which yields the highest T_c's. Since the x rays show that over most of this range the predominant phase is A-15, we conclude that compositions yielding the best T_c require formation at the lowest temperatures. The T_D-vs-composition results also indicate that for films deposited with a range in composition the optimum T_D will cover a range in temperatures making this parameter only slightly less critical than for fixed composition sputtering. This will not explain, however, all of the differences among the reported optimum T_D's and their ranges.[4-8]

Electrical resistivities of films deposited at the optimum T_D over the composition range studied generally fall in the range ~70–110 $\mu\Omega$ cm at 300 K and ~30–110 $\mu\Omega$ cm at 25 K (see Fig. 6). Uncertainties are ~25% and due mainly to film thickness uncertainty and nonuniformity. Variations of ρ with film thickness between 2000 and 20 000 Å is generally $\leq 50\%$. The resistance ratio $\rho(300\text{ K})/\rho(25\text{ K})$ at optimum T_D, which can be determined with an error $\leq 3\%$, is also shown as a function of composition in Fig. 6. Again we find a minimum in ρ and a maximum in resistance ratio for Nb/Ge ~2.8–3.

For films which have been deposited at (700–800)°C the resistivities are quite high and correspond to electron mean free paths at 25 K of only ~50 Å. Note that considerably away from the 3/1 composition the resistance ratios are ~1, indicating solution disorder rather than a mixture of ordered phases. The data shown in Fig. 6 are typical values, but the highest resistance ratio obtained to date is only ~3, this occurring for films with T_c ~23 K. The significance of these low ratios becomes evident when we compare them with values for A-15 bulk materials which are generally in the range 10–100. Our films are sufficiently thick compared to the mean free path (or superconducting coherence length) to preclude complications from two-dimensional effects. At these high deposition temperatures the grain size is relatively large (x-ray lines observable out to $2\theta = 135°$), and the impurities found in these films are insufficient to account for such short mean free paths. It thus appears that alloy-disorder defects or microscopic defects are the principle cause of the high resistivities and that even in the range of the 3/1 composition these effects limit the electron mean free path to considerably less than what one achieves in the bulk. How this may, in turn, relate to the superconducting T_c is shown in the simple correlation described in Sec. III G.

G. Correlation of resistance ratio and T_c

Figure 7 presents a sampling of T_c-vs-resistance-ratio data for about 130 films and is representative, in fact, of almost all samples obtained in the present study. The data points are given here irrespective of sputtering voltage, deposition temperature, deposition rate, argon pressure, film thickness, crystal structure, and even chemical composition through most of the

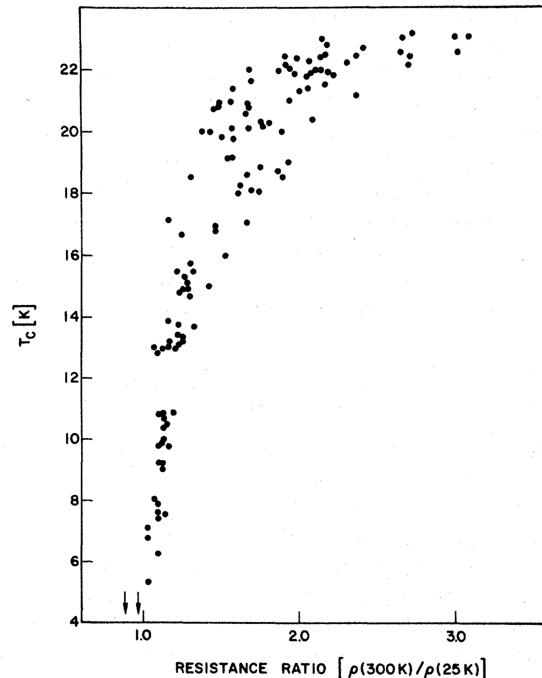

FIG. 7. Correlation of electrical resistance ratio with T_c. The data points relate to films made with various sputtering voltages and currents, deposition rates, and deposition temperatures and having different thickness, x-ray structures, and chemical composition.

range Nb/Ge ~2.4–5.5. The only restriction in choosing points for this plot was that the width of the superconducting transition be less than ~2–3 K, thereby insuring that those films which were grossly inhomogeneous, by this criterion, were excluded.

Note that within the scatter there is a reasonable correlation between T_c and the resistance ratio. Resistance ratios less than 1 generally occur in films which are not superconducting. However, an increase in resistance ratio up to only 1.3 is sufficient to yield T_c's of ~15 K, and resistance ratios of 2–3 are generally accompanied by superconductivity between 21 and 23 K. If the resistance ratio is controlled by disorder, defect, or strain scattering, as conjectured above, this correlation strongly suggests that this mechanism is more critical in controlling T_c than is indicated by the composition alone and, furthermore, that this mechanism is not markedly reduced at the 3/1 composition ratio.

The mean free paths estimated for the best films at low temperatures are grossly ~50 Å, which is probably not much different than the superconducting coherence length. Thus the superconducting properties may be (detrimentally) averaged by microscopic conditions still unknown.

The steepness of the resistance-ratio–T_c correlation in Fig. 7 seems to be diminishing at high T_c's, although the reduction in data points there–only five or six films with T_c's of ~23 K—makes it difficult to determine this quantitatively. Nevertheless, it would appear important to determine why the mean free paths are so short. It is possible that sputtered films may have not yet achieved the highest possible T_c's for Nb-Ge. What remains to be done probably must, in some way, lead to increases in the resistance ratio. Whether this means increased order or decreased defects or some yet unrecognized property is still not known.

H. Variation of properties and structure with deposition temperatures

In the interval of deposition temperature between 640 and 740°C large changes occur in the superconducting T_c, electrical resistivity, resistance ratio, and x-ray structure. Figures 8 and 9 show how some of these properties vary for six films deposited simultaneously in two runs (using different targets) where the average chemical composition Nb/Ge was ~3 and ~2.7. For these films the sputtering voltage was 600 V, argon pressure 200 mTorr, and the deposition rate ~20 Å/min. The data show that between 640 and 740°C the T_c increases from less than 4.2 K (the lowest temperature for measurement) to ~22 K. Resistivities at 300 K generally decreased from ~120 to ~80 μΩ cm and resistance ratios increased from ≤1 to ~2 over this T_D interval. X-ray diffraction studies showed an amorphous structure at T_D= 640°C, which gave way to a predominantly *A*-15 structure at the higher T_D's. This is in agreement with the previously reported results of Chencinski and Cadieu[7] and Ghosh *et al.*[8]

Rutherford backscattering data show that these large changes are not accompanied by marked variances in the overall chemical composition of the films. From the discussion in Sec. III D it is also seen that the observed variations in Nb/Ge ratio are too small to account for the T_c behavior. We conclude that crystallographic and/or other microscopic changes are primarily responsible for the different physical behavior.

The analysis of this type of alloy sputtering is often compromised by assumptions about relative sputtering efficiencies and, of greater concern, relative sticking coefficients, and how they might vary with T_D (or film structure). The Rutherford data bypass these complications and show that film composition doesn't vary appreciably with T_D. The small variations in Nb/Ge which are seen in Figs. 8 and 9 are not systematic in the two cases and may be partly the remanence of gross target inhomogeneities (~30%) which have been found with x-ray fluorescence.

I. Bias and magnetic-field-assisted sputtering

Films were prepared with the substrate table held at positive and negative dc bias potentials relative to ground (the can in Fig. 1). The diffuse

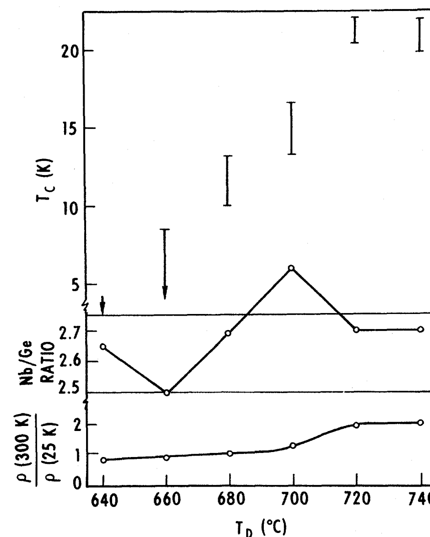

FIG. 8. Variation of T_c, Nb/Ge ratio, and electrical resistivity ratio with deposition temperature.

nature of sputtering establishes a conducting path from the table to the substrate surfaces soon after deposition begins; so the bias potentials occur at the growing film surface. Sputtering voltage, deposition temperature, and argon pressure were maintained near the optimum values (at no bias) of 600 V, 740°C, and 200 mTorr, respectively.

The largest effect on the superconducting behavior occurred for negative bias, which lead to reductions in T_c from ~2 to 10 K compared to the no-bias result. Bias voltages of −45 and −90 V were used, and no current greater than several mA was detected in the bias circuit during sputtering. These large changes in T_c occurred with little, if any, variation in the sputtering current or the deposition rate. The reductions in T_c were different in the two sputtering systems and may, therefore, depend on the geometry of the environment and the relative size of the sputtering target. X-ray flourescence measurements of films made with and without bias showed that the Nb/Ge ratio was the same to within ~5−10%, which is about the reliability of this determination.

Positive bias (+30 to +100 V) was accompanied by currents ~30−100 mA in the bias circuit but no appreciable change in T_c, although the sputtering current and perhaps the deposition rate were increased slightly. (The bias current may be due to ejected target electrons collected by the substrate.) It would appear from limited testing that positive bias has no detrimental effect but may lead to slightly less critical adjustments of the sputtering conditions for high T_c's, and, in addition, a small increase in sputtering rates particularly at low voltage.

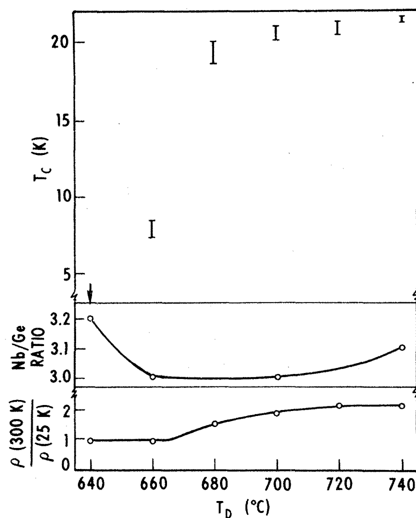

FIG. 9. Variations of T_c, Nb/Ge ratio, and electrical resistivity ratio with deposition temperature. (Data of Figs. 8 and 9 obtained with different targets.)

Since the detailed studies of T_c vs composition show that chemical variations of ~(5−10)% have negligible effect on T_c, we conclude that some aspect of the structure or impurity content is being altered by the use of negative bias. It is possible that negative bias attracts some of the energetic ions which may damage or prevent in some way the growth of the high-T_c phase. But from the present studies no conclusions can be drawn.

Sputtering has also been carried out using magnetic fields of 200−1000 Oe applied parallel and perpendicular to the substrate surfaces. T_c onsets of ~21 K were obtained in most cases, but, particularly for the parallel-field case, a peculiar pattern of shading was observed on both the films and the target. The major effects of magnetic field sputtering were (i) a marked increase (sometimes exceeding a factor of 2) in sputtering current and deposition rate particular at low voltage (e.g., ~30 Å/min at 330 V could be obtained with magnetic fields) and (ii) an increase in the optimum deposition temperature by ~200°C. The first result is not too surprising and, indeed, points to a simple way to get reasonable deposition rates at very low voltages. The second effect is quite unexpected and no explanation is available. The shift in optimum T_D with magnetic field seems well outside of our error in determining this temperature and is opposite to what could be expected from heating due to the increased sputtering rate. The magnetic field should lead only to changes in the trajectories of the ions or the ejected electrons in the sputtering atmosphere. How these changes can significantly alter the temperature at which the high-T_c phase is formed is not understood. Although an independent method of varying the optimum T_D in sputtering would be useful, it is not known in which direction the change would be beneficial for T_c.

The bias and magnetic field sputtering studies described here were preliminary in nature, and extensive attempts to optimize T_c have not been made. Composition and x-ray studies of the films were not carried out. It would appear, however, that one or both variants may be useful in the sputtering process, if only to increase the sputtering rate. The shift in T_D with magnetic field shows again the complexity (and the versatility) of the sputtering process; an understanding may yet yield further processing control.

J. Substrate strain effects

A significant unknown in all of the Nb-Ge sputtered film work is the effect on the properties of the strains present in the film. A simple calculation shows that this problem may not be trivial.

If the difference in average thermal expansions of A-15 Nb-Ge and Al_2O_3 (which gives the highest T_c's) is only 1×10^{-6} °C^{-1} between 0 and 1000 K, then strains $\sim10^{-3}$ will be present in the films at low temperatures. Furthermore, such strains, because of the film-substrate geometry, may be partly of the tetragonal type—the most influential—and probably detrimental for T_c. All high-T_c A-15 superconductors have now been reported to show low-temperature structural transformations. These are accompanied by tetragonal strains $\sim10^{-3}$, which *per se*, cause a depression in T_c of ~1 K. The highest T_c's (~23 K) can be reproduced only with difficulty (~5–6 such films have been made in this study). Although nonuniformities in the sputtering conditions may be partly responsible for this, the variations in the strain may also be of importance. It should be noted that Al_2O_3 (thermal expansion ~5 to 10×10^{-6}°C^{-1} between room temperature and 800°C) is hexagonal with an anisotropy $\sim1\times10^{-6}$C^{-1} in the thermal expansion (the thermal expansion of A-15 NbGe is not known). Since our substrates are single crystals of random orientation, the strain effects, in addition, may not be quite reproducible.

One further comment on strain effects is that from the x-ray data and the composition-vs-T_c data of Fig. 5 we know that for the bulk A-15 composition Nb/Ge ~4; we obtain $T_c\sim14$ K and $a_0\sim5.14$ Å in the films. This should be compared to $T_c\sim6$ K and $a_0\sim5.168$ Å obtained in bulk. Thus thin films give a higher T_c and a smaller lattice parameter compared to the bulk for the same composition. It seems unlikely that the very great increase in T_c is directly the result of the smaller lattice parameter. Although smaller lattice parameters are generally a good indicator of higher-T_c samples even for bulk Nb_3X superconductors, for the films substrate-strain effects on T_c may be present on a smaller but significant scale. Gavaler *et al.*[6] have recently reported that the lattice parameter of high-T_c Nb-Ge on the substrate was $\sim2\times10^{-3}$ smaller than when removed from the substrate. To determine the effect of this on T_c requires T_c measurements on and off the substrate performed in the same manner (e.g., inductively). No measurements have been reported.

Substrate (tetragonal) strain effects would probably also reduce the likelihood of a Batterman-Barrett transformation occurring at low temperatures in these films. X-ray measurements for a single sample showed no change in the diffraction-line positions or widths between 300 and ~15 K. Further experiments, particularly of the anomalous linewidth behavior, are planned.

Finally, it should be noted that in thin films the "intrinsic" strains discussed above are generally exceeded by "extrinsic" strains (unrelated to thermal expansion) whose origins are complicated and not fully understood.[22]

IV. CONCLUSIONS

The deposition of NbGe onto hot substrates using low-energy sputtering has allowed the formation of the A-15 phase over a far wider range in composition than that achieved in normal bulk sample preparations. It is still unknown, however, if this results from the low temperature of formation for the films or whether this is due, in some way, to the two-dimensional (layer-by-layer) growth process which occurs for the film samples. Dew-Hughes[28] has pointed out that the thermodynamics of the competing phase—Nb_5Ge_3 in our case—is important in determining whether stoichiometric A-15 compounds can be formed. Thus one interpretation of the Nb-Ge results would place the free energy of *D8m* Nb_5Ge_3 somewhat below that for A-15 Nb_3Ge near the melting point (~2000°C) but in reverse order below ~1000°C. This would allow the formation of A-15 Nb_3Ge only at low temperatures. For Nb-Ge and Nb-Ga a similar shift of the A-15 phase toward the 3/1 composition has been shown in the work of Hammond[23] and Webb,[24] respectively. The kinetics of this reaction may well be too slow in the bulk but greatly enhanced in the films where surface diffusion can control the growth. Thus, both the low formation temperature and the surface reactions may be important in the film samples.

Several other observations, however, show that the problem of the competing phase may have implications beyond what is indicated above. The Rutherford and x-ray studies show that films deposited at ~640°C, which are not superconducting, have an amorphous structure and contain approximately several percent O and C. For T_D ~740°C, which yields high T_c's, the A-15 crystalline structure containing considerably less C and O is obtained. A probable explanation is that T_D ≈640°C is too low to form the crystalline phase, and the resulting amorphous phase—perhaps by enhanced absorption or diffusion during growth—allows more of the ambient impurities to be incorporated. A less likely, but more serious possibility, is that the kinetics for O and C absorption are higher at 640 than 740°C (irrespective of structure) and the amorphous phase is stabilized by the presence of the impurities. If this is true, it represents an important and (for T_c) detrimental limitation to the formation A-15 Nb_3X compounds at low temperatures by these techniques.

Although the sputtered films have yielded the

A-15 structure over a wide compositional range, the compositional studies have shown that the formation of exactly stoichiometric A-15 structure films is not necessary for high T_c's. For compositions similar to those in bulk material the films have higher T_c's and smaller lattice parameters. Thus some other feature of the microstructure, important for T_c, is being favored in the film growth. The resistance-ratio–T_c correlation provides a clear signature of this feature, but its identity, as yet, is unknown.

Finally, the discussion of higher T_c's brings us unavoidably to Nb_3Si. Although various extrapolations suggest T_c's of ~25–38 K,[26] the bulk material (Cu_3Au structure) shows ~1 K or less. Evaporated[25] and sputtered[3,27] films of Nb_3Si have been obtained with A-15 and tetragonal structures and having T_c onsets of ~7–9.9 K. The competing Nb_5Si_3 phase here may be even more serious than for Nb_3Ge. By chemical additions, growth technique, or lower formation temperature one must disfavor the formation of this phase (and other competing phases) and obtain, hopefully, a phase similar to what has produced high T_c's in Nb-Ge.

ACKNOWLEDGMENTS

The authors are greatly indebted to J. E. Bernardini for preparation of the targets, K. Bachman and J. Rubin for the zone refining of Nb, S. C. Abrahams for the single-crystal x-ray study of the Nb_5Ge_3 target, and W. M. Augustyniak for assistance with the accelerator.

[1]For a list of recent references and a discussion of this behavior in A-15 compounds see L. R. Testardi, Rev. Mod. Phys. (to be published).
[2]L. R. Testardi, J. J. Hauser, and M. H. Read, Solid State Commun. 9, 1829 (1970).
[3]L. R. Testardi, J. H. Wernick, W. A. Royer, D. D. Bacon, and A. R. Storm, J. Appl. Phys. 45, 446 (1974).
[4]J. R. Gavaler, Appl. Phys. Lett. 23, 480 (1973).
[5]L. R. Testardi, J. H. Wernick, and W. A. Royer, Solid State Commun. 15, 1 (1974).
[6]J. R. Gavaler, M. A. Janocko, and C. K. Jones, J. Appl. Phys. 45, 7 (1974).
[7]N. Chencinski and F. J. Cadieu, J. Low Temp. Phys. (to be published).
[8]A. K. Ghosh, L. Pendrys, and D. H. Douglass, in Proceedings of the 1974 Applied Superconductivity Conference, Chicago (to be published).
[9]J. H. Carpenter and A. W. Searcey, J. Am. Chem. Soc. 78, 2079 (1956).
[10]S. Geller, Acta Crystallogr. 9, 885 (1956).
[11]B. T. Matthias, T. H. Geballe, R. H. Willens, E. Corenzwit, and G. W. Hull, Jr., Phys. Rev. 139, A1505 (1965).
[12]B. T. Matthias, T. H. Geballe, L. D. Longinotti, E. Corenzwit, G. W. Hull, Jr., R. H. Willens, and J. P. Maita, Science 156, 645 (1967).
[13]*Gmelins Handbuch der Anorganischen Chemie* (Verlag, Weinheim, 1971), Vol. B2, p. 201.
[14]J. W. Mayer and J. F. Ziegler, *Ion Beam Surface Layer Analysis*, edited by J. W. Mayer and J. F. Ziegler (Elsevier Sequoia, New York, 1974).
[15]H. C. Theurer and J. J. Hauser, Trans. Metall. Soc. AIME 233, 588 (1965).
[16]Also confirmed by S. C. Abrahams on a single crystal chip obtained from the ingot.
[17]J. M. Poate and T. M. Buck, *Experimental Methods in Catalytic Research*, edited by R. B. Anderson and P. T. Dawson (to be published).
[18]M. A. Nicolet, I. V. Mitchell, and J. W. Mayer, Science 177, 841 (1972).
[19]For an interesting correlation of T_c and the compositional width of the A-15 phase in other materials see F. E. Wang, J. Phys. Chem. Solids 35, 273 (1974).
[20]J. S-Y. Feng, W. K. Chu, and M-A. Nicolet, Thin Solid Films 19, 227 (1973).
[21]L. C. Northcliffe and R. F. Schilling, Nucl. Data Tables 7, 233 (1970).
[22]See K. L. Chopra, *Thin Film Phenomena* (McGraw-Hill, New York, 1969), p. 266.
[23]R. H. Hammond, in Ref. 8.
[24]G. W. Webb and J. J. Engelhardt, in Ref. 8.
[25]R. H. Hammond and S. Hazra, *Low Temperature Physics-LT13*, edited by K. D. Timmerhaus, W. J. O'Sullivan, and E. F. Hammel (Plenum, New York, 1974), p. 465.
[26]D. Dew-Hughes and V. G. Rivlin, Nature 250, 723 (1974).
[27]G. Johnson and D. H. Douglass, J. Low Temp. Phys. 14, 575 (1974).
[28]D. Dew-Hughes (unpublished).